JOURNAL OF MATERIALS SCIENCE 13 (1978) 1794–1804

Microstructure and properties of transparent glass-ceramics

Part 2 *The physical properties of spinel transparent glass-ceramics*

A. J. STRYJAK, P. W. McMILLAN
Department of Physics, University of Warwick, Coventry, UK

The variation of a number of physical properties of certain transparent glass-ceramic compositions as a function of the crystallization heat treatment is reported. The properties studied include thermal expansion, hardness, mechanical strength and transmission in the visible and near infra-red regions. It is shown for one of the spinel transparent glass-ceramics chosen for a detailed investigation, that most of the properties are dependent on the microstructural effects.

1. Introduction

The variation of microstructure with heat treatment of a spinel transparent glass-ceramic based on the $ZnO-Al_2O_3-SiO_2$ system has been previously reported by the authors [1]. In the present paper the physical properties are described and compared with the statistical description of the microstructure. The physical properties measured are the coefficient of thermal expansion, microhardness, modulus of rupture and Young's modulus, and optical transmission in the visible and near infra-red range.

2. Apparatus and methods

2.1. Thermal expansion measurements

The coefficients of thermal expansion of the glasses and glass-ceramics were measured on a silica dilatometer. This consisted of a fused silica specimen holder and a linear variable differential transformer (LVDT). The LVDT produced an electrical signal proportional to the linear displacement of its core. The specimen holder was positioned vertically in a furnace and the expansion of the specimen was transmitted via a silica push rod to the core of the LVDT. The LVDT and the top of the push rod were kept at a constant temperature by passing water at 25° C around the system. Samples approximately 5 cm in length were used. Five specimens of each material were measured.

2.2. Mechanical properties

The modulus of rupture and Young's modulus in bending of the glasses and glass-ceramics were determined by a three-point bending technique. A three-point bending jig with a 2 cm span between the outer knife edges was used on an Instron Universal Testing machine operating at room temperature and at a cross-head speed of 0.02 cm min^{-1}. On average eight specimens were used for each strength measurement. Specimens were initially given a standard surface abrasion but proved to give unsatisfactory results. Therefore, some specimens were given a mild abrasion before heat treatment, and others received no abrasion at all.

The specimens which were abraded received the standard abrasion treatment of 60 min in a rotary ball-mill containing $\leqslant 100$ mesh Carborundum powder in an amount corresponding to 20 times the weight of the specimens. The samples abraded before heat treatment received the above treatment for 5 min.

Rectangular beams were used in the measurements having dimensions of approximately 25 mm × 5 mm × 3 mm.

The modulus of rupture, σ_F, of a rectangular bar for centre loading is determined from the expression

$$\sigma_F = \frac{3P_F L}{2bd^2}$$

where P_F is the load to fracture, L is the distance between the outer knife edges, b is the width of the sample, and d is the thickness of the sample.

Young's modulus in bending, E_b, is determined from the force–deflection curve arising from the expression

$$E_b = \frac{PL^3}{4bd^3Y}$$

where Y is the deflection corresponding to a load P.

The microhardness was measured by the Vickers diamond pyramid test for glass and glass-ceramics specimens. The hardness, H_v, is defined as

$$H_v = \frac{2P \sin \alpha/2}{D^2}$$

where P is the indenting load, D is the mean value of the impression diagonal, α is the 136° angle between opposite indenter faces.

The diamond indenter was incorporated in a McCrone microhardness apparatus mounted on an inverted optical microscope. Indentations were made on the surfaces of glass and glass-ceramic specimens polished to a 1 μm diamond paste finish.

Ten indentations were made for each specimen with a time of 15 sec at full load of a 1000 g weight.

2.3. Optical transmission measurements

Optical transmission spectra were recorded in the ultra-violet range (250 nm to 400 nm) and in the visible region (350 nm to 750 nm) on a Perkin Elmer III Spectrometer, and in the infra-red region (0.5 μm to 6 μm) on a Grubb Parsons Infra-red spectrometer.

Samples approximately 1 mm in thickness were polished on both sides using 6 and 1 μm diamond pasted pads.

3. Results

The glass-ceramics referred to in the following sections were crystallized from the parent glasses whose compositions have been given previously in [1]. The heat treatment schedule for the determination of physical properties was 800° C for 4 h and 950° C 1 to 6 h for all glasses 1, 2, 3 and 4.

3.1. Thermal expansion

Table I gives a summary of thermal expansion coefficients of the above glasses and glass-ceramics. It can be seen that glass 1 has an expansion coefficient of $21.4 \times 10^{-7\circ} C^{-1}$, whereas the glass-ceramic has an expansion coefficient of $12.4 \times 10^{-7\circ} C^{-1}$. It is known that β-quartz s.s. has a very low expansion coefficient: approximately $5 \times 10^{-7\circ} C^{-1}$ [2], indicating that overall the glass-ceramics should produce a lower expansion than the parent glass, even though there is present a low volume fraction of tetragonal zirconia crystals having a high expansion coefficient of $\sim 128 \times 10^{-7\circ} C^{-1}$ [3]. Fig. 1 shows percentage expansion curves of the glasses and glass-ceramics 1, 2, 3 and 4. The expansion increases from glass 1 to 2 to 3 to 4. For glass 1 to have a lower expansion than the other would be expected, since the extra amount of ZrO_2 in glass 2 would increase the overall expansion. The increase in expansion from glass 2 to 3 to 4 is also expected due to the presence of larger alkaline earth metal ions. The size of the ions increases from Mg^{2+} to Ca^{2+} to Ba^{2+} with a corresponding decrease in ionic field strength.

TABLE I Thermal expansion coefficients of glasses and glass-ceramics (20 to 800° C)

Composition no.	$\alpha(\times 10^{-7\circ} C^{-1})$ Base glass	$\alpha(\times 10^{-7\circ} C^{-1})$ Glass-ceramic 800° C 4 h 950° C 4 h
1	21.4 ± 0.2	12.4 ± 0.2
2	23.1 ± 0.2	26.6 ± 0.2
3	25.5 ± 0.1	31.0 ± 0.1
4	26.9 ± 0.3	38.1 ± 0.3

TABLE II Thermal expansion coefficients of glass 3 after various heat treatments

Glass 3	$\alpha(\times 10^{-7\circ} C^{-1})$ 20–800° C	$\alpha(\times 10^{-7\circ} C^{-1})$ 400–800° C
Base glass	24.4 ± 0.1	28.9 ± 0.1
800° C 4 h–950° C 1 h	24.5 ± 0.2	25.9 ± 0.2
800° C 4 h–950° C 2 h	27.9 ± 0.1	29.3 ± 0.1
800° C 4 h–950° C 3 h	28.8 ± 0.3	30.3 ± 0.3
800° C 4 h–950° C 4 h	31.0 ± 0.1	33.1 ± 0.1
800° C 4 h–950° C 5 h	31.7 ± 0.09	33.8 ± 0.09
800° C 4 h–950° C 6 h	31.5 ± 0.3	33.6 ± 0.3

Table II and Fig. 2 shows the percentage expansion of glass 3 as a function of extent of crystallization. The steady increase in the expansion is due to the growth of gahnite crystals, gahnite having an expansion coefficient of approximately $77 \times 10^{-7\circ} C^{-1}$ [4]. The maximum expansion appears to be attained after approximately 4 h at the crystallization temperature, when the maximum size and volume fraction of gahnite crystals has been reached [1].

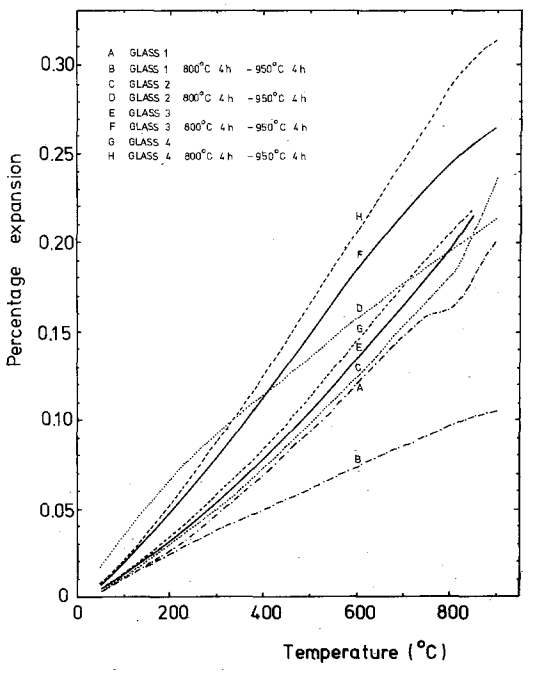

Figure 1 Percentage expansion curves of glasses and glass-ceramics 1, 2, 3 and 4.

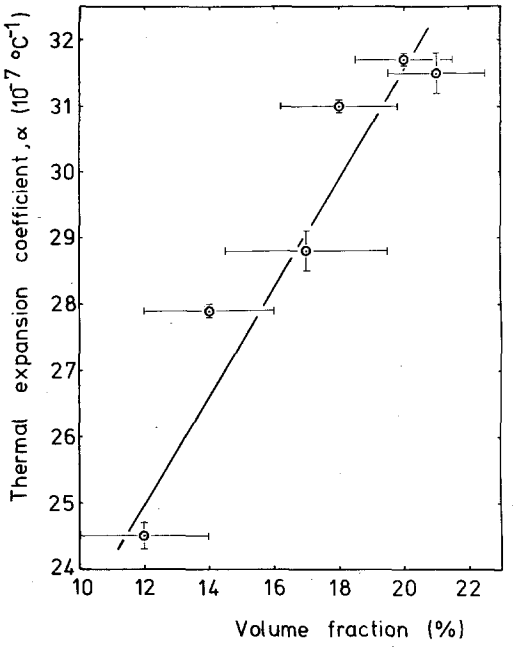

Figure 3 Variation of expansion coefficient, α, with volume fraction, V_f, of gahnite crystals in glass-ceramic 3.

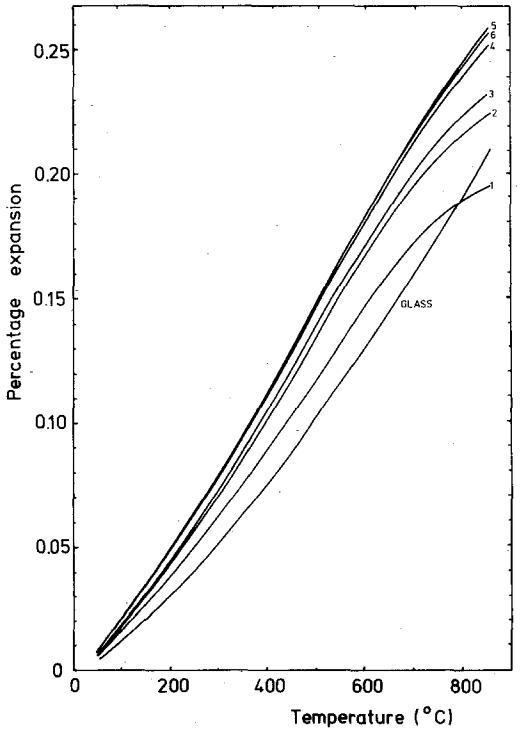

Figure 2 Percentage expansion curves of glass 3 after various heat treatment times (the numbers on the right of the curves refer to the number of hours the samples had been heat treated at 950° C after a nucleation treatment of 800° C for 4 h.)

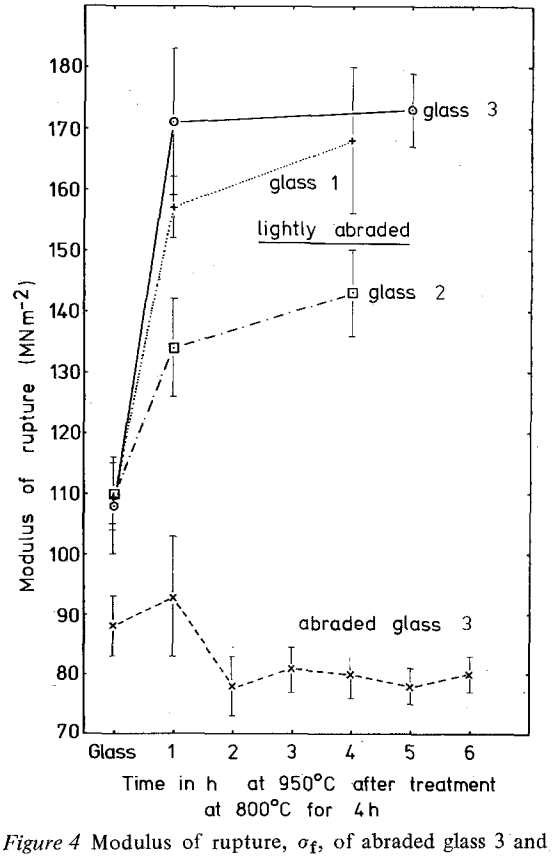

Figure 4 Modulus of rupture, σ_f, of abraded glass 3 and lightly abraded glasses 1, 2 and 3 for various heat treatments.

Fig. 3 shows the change in thermal expansion coefficient with the volume fraction of gahnite crystals present in glass-ceramic 3.

3.2. Mechanical properties

3.2.1. Modulus of rupture

The modulus of rupture by three-point bending of abraded samples of heat-treated glass 3 gave very scattered results with no apparent dependence on the microstructure, as shown in Fig. 4. It is suspected that the lack of dependence on the microstructure of glass-ceramic 3 can be attributed to the introduction of cracks and flaws during abrasion which are larger than the average particle size. Further work on selected heat treatments of glasses 1, 2 and 3 with much shorter abrasion times produced the results of Fig. 4. It can be seen that the moduli of rupture of the parent glasses all lie within the range 108 to 110 MN m^{-2}. Subsequent crystallization led to a large increase in the moduli of rupture, which then appeared to stabilize. The large errors involved in the measurements of the moduli of rupture made it impossible to achieve a relationship with respect to the microstructural parameters.

Further work on omitting the abrasion treatment and also of increasing the span-to-depth ratio of test specimens [5] of glass-ceramic 3 produced the results of Fig. 5. The overall strength of the glass-ceramic can be seen to decrease. It can also be seen that there is a significant difference between the overall strength of abraded and unabraded crystallized glass 3. It would be expected for the unabraded samples to have a higher strength than the abraded ones, because of the larger number of flaws introduced onto the surface during the abrasion process. It must be remembered, however, that for smaller span-to-depth ratio (abraded specimens) shearing forces could have given a higher value of the strength. Essentially, therefore, the results of Fig. 4 cannot be used for strength–microstructure determinations.

Fig. 6 shows the relationship between the strength of glass-ceramic 3 and the square root of the particle size, the line of best fit being drawn in after a least squares calculation. The large errors associated with both modulus of rupture and particle size measurements make it difficult to establish this relation.

The relationship that strength is proportional to $d^{-1/2}$ would indicate that the initial flaws are present at the glass–crystal interface, because of stresses introduced at these boundaries, due to the thermal expansion difference between the glass

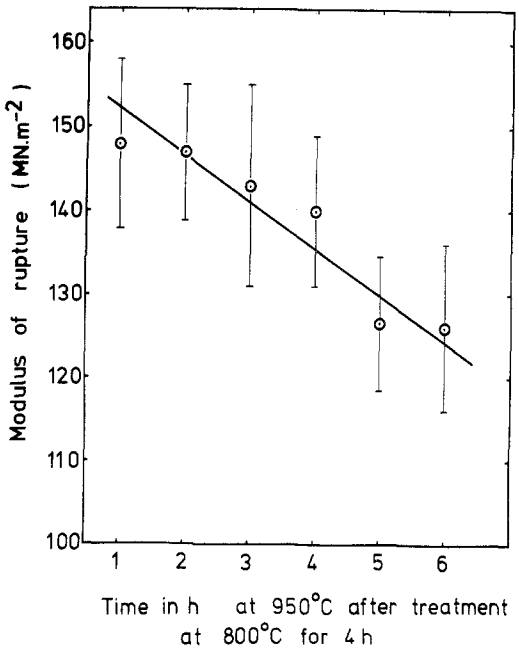

Figure 5 Modulus of rupture, σ_f, of unabraded glass 3 after various heat treatment times (Note that the parent glass has been omitted).

and crystal phases. Tashiro and Sakka [6] pointed out the interdependence between the modulus of rupture, σ_F, of the glass-ceramic and the thermal expansion coefficient of the primary crystal phase. McMillan [7] has suggested that where the thermal expansion coefficient of the crystal phase is very much lower than that of the glass phase, the stresses in the glass phase around a crystal will be tensile in the circumferential direction and compressive in the radial direction. In such a material, microcracks aligned with their major axes in the radial direction, are likely to be most critical, and thus predicts that the dependence of strength on $\lambda^{-1/2}$ is likely to be applicable, where λ is the mean free path between crystals. Where the thermal expansion coefficient of the crystal phase is higher than that of the glass, which is the case in the present study, the stresses in the glass immediately surrounding the crystal will be compressive in the circumferential direction and tensile in the radial direction. Thus microflaws having their major axes aligned in the circumferential direction are likely to be more critical in this case. For such materials, therefore, microcracks formed at the grain boundaries rather than those traversing the glass phase may be the controlling factor. The lengths of these flaws will be proportional to the crystal diameter, d, and hence a dependence of the strength upon $d^{-1/2}$ might be expected.

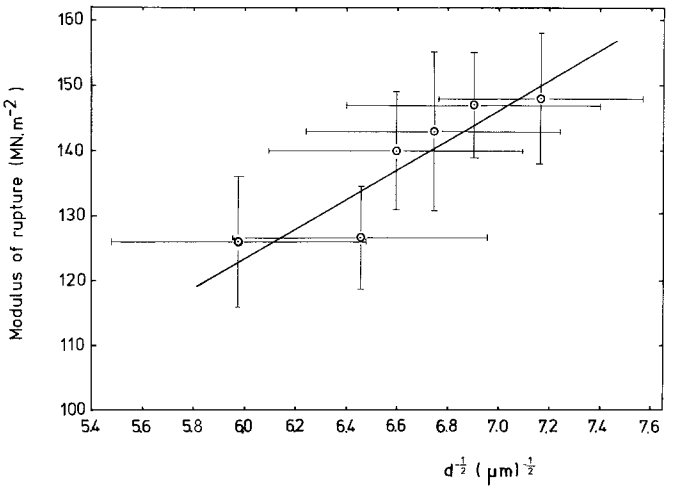

Figure 6 Dependence of the modulus of rupture, σ_f, upon the square root of the mean crystal size of glass-ceramic 3.

Agreement, therefore, exists between the present work and the results of McMillan [7], whereby the expansion coefficient of the gahnite phase was much higher than the residual glass phase leading to the dependence of strength and $d^{-1/2}$.

3.2.2. Young's modulus

From the series of tests performed on the unabraded samples of glass-ceramic 3, load–deflection curves were analysed to determine Young's modulus. Fig. 7 shows that the parent glass has a Young's modulus of $(4.1 \pm 0.2) \times 10^{10}$ Nm^{-2}. This value then remains constant for the remainder of the heat treatment schedule. Although the modulus of elasticity is an additive function of the individual characteristics of the crystalline and glassy phases, there appears to be no change in the value of E_b during the crystallization process, evidently because of the small change in the volume fraction of the crystal species.

Table III gives a summary of the mechanical strength measurements.

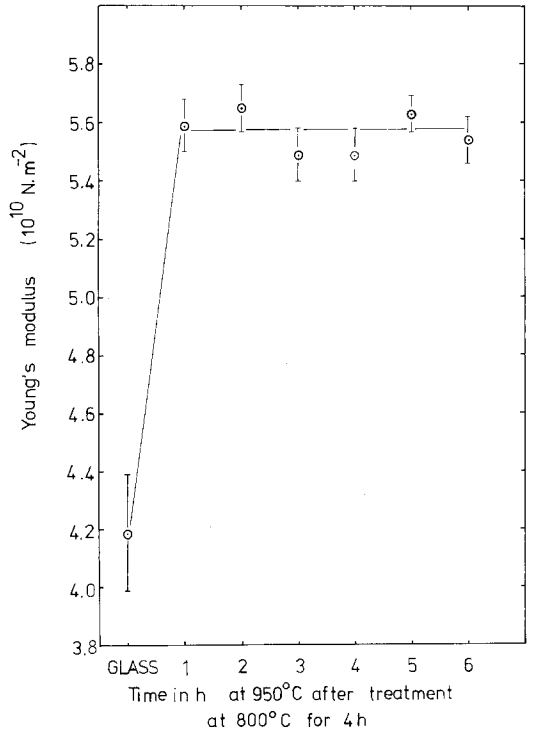

Figure 7 Young's modulus of glass 3 after various heat treatment times.

3.2.3. Microhardness

Hardness measurements were performed on glasses 1, 2, 3 and 4 before and after various heat treatments.

Table IV and Fig. 8 show the results of hardness measurements on glass and glass-ceramic 3, subjected to both nucleation and crystallization heat treatments. Two facts are apparent from the figure;

(a) The nucleated glasses have a lower hardness than the parent glass. The hardness rises to a maximum after three hours and decreases again. No microstructural changes were observable in the nucleated glasses by electron microscopy and so no change was expected in the microhardness of these glasses. The decrease in the hardness of these nucleated glasses may arise from the crystallization of tetragonal zirconia which shows a high hardness of approximately 1100 VHN (kg mm^{-2}) [8], resulting in a decrease in the hardness of the glassy matrix. The volume fraction of tetragonal zirconia being only 9% would not be sufficient to raise the overall hardness.

(b) In the crystallization region, the microhardness rises linearly up to a 4 hour treatment and

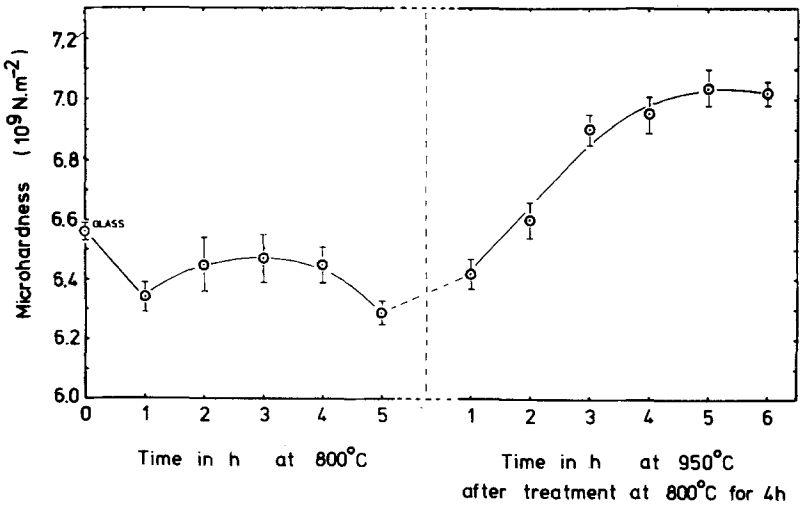

Figure 8 Microhardness of glass 3 after various heat treatment times.

subsequently levels off after a 5 to 6 hour treatment. The increase is, as expected, due to the high hardness of gahnite, which is approximately 1300 VHN [8].

Table V shows a comparison of the hardness measurements of glasses 1, 2, 3 and 4 and their corresponding glass-ceramics. The parent glasses all fall within a narrow range, but the glass-ceramics show a wider variation. Fig. 9 relates the microhardness of glass-ceramics 3 to glass-ceramic 1. It is apparent that the high hardness of glass-ceramic 1 is due to the high volume fraction of β-quartz crystals.

Fig. 10 shows the relationship between the microhardness and volume fraction of gahnite crystals in glass-ceramic 3.

In relation to the crystal microstructure, it is apparent that some relationship exists between the hardness and crystal size. A theoretical relationship derived by Stroh [9] assumes a hardness proportional to $d^{-1/2}$, where d is the average particle size, if the deformation in a polycrystalline aggregate is caused by slip within grains. If a slip occurs at grain boundaries, however, Zener [10] revised the equation to $H_v = \text{constant } d^{+1}$, because in this case the tendency for slipping increases in proportion to the total area of the grain boundaries.

Fig. 11 indicates that the measured values of hardness of glass-ceramic 3 for various heat treatments are proportional to the average particle size. This would indicate that the fracture mechanism occurs at grain boundaries. This conclusion was hard to justify due to the large errors associated with the measurement of the small particle size. The line of best fit was drawn after a least squares calculation.

TABLE III Mechanical strength measurements of selected glasses and glass-ceramics

Material	σ_f(Mn m^{-2}) (samples abraded for 60 min)	σ_f(MN m^{-2}) (samples abraded for 5 min)	σ_f(MN m^{-2}) (unabraded)	Young's modulus E_b (10^{10} N m^{-2})
Glass 3	88 ± 5	108 ± 8	108 ± 8	4.1 ± 0.2
800° C 4 h 950° C 1 h	93 ± 10	171 ± 12	148 ± 10	5.6 ± 0.9
800° C 4 h 950° C 2 h	78 ± 5	–	147 ± 8	5.65 ± 0.8
800° C 4 h 950° C 3 h	81 ± 4	–	143 ± 12	5.5 ± 0.9
800° C 4 h 950° C 4 h	80 ± 4	–	140 ± 9	5.5 ± 0.9
800° C 4 h 950° C 5 h	78 ± 3	173 ± 6	126.5 ± 8	5.6 ± 0.6
800° C 4 h 950° C 6 h	80 ± 3	–	126 ± 10	5.5 ± 0.8
Glass 2	–	110 ± 5	–	–
800° C 4 h 950° C 1 h	–	134 ± 8	–	–
800° C 4 h 950° C 4 h	–	143 ± 7	–	–
Glass 1	–	110 ± 6	–	–
800° C 4 h 950° C 1 h	–	157 ± 5	–	–
800° C 4 h 950° C 4 h	–	168 ± 12	–	–

TABLE IV Microhardness of glass 3 after various heat treatments

Material	H_v (kg mm^{-2}) VHN	H_v (10^9 N m^{-2})
Base glass	669 ± 3	6.56 ± 0.03
800° C 1 h	646 ± 5	6.34 ± 0.05
800° C 2 h	658 ± 10	6.45 ± 0.09
800° C 3 h	660 ± 8	6.47 ± 0.08
800° C 4 h	658 ± 6	6.45 ± 0.06
800° C 5 h	641 ± 4	6.29 ± 0.04
800° C 4 h 950° C 1 h	655 ± 5	6.42 ± 0.05
800° C 4 h 950° C 2 h	673 ± 6	6.60 ± 0.06
800° C 4 h 950° C 3 h	704 ± 5	6.90 ± 0.05
800° C 4 h 950° C 4 h	709 ± 6	6.95 ± 0.06
800° C 4 h 950° C 5 h	718 ± 6	7.04 ± 0.06
800° C 4 h 950° C 6 h	716 ± 4	7.02 ± 0.04

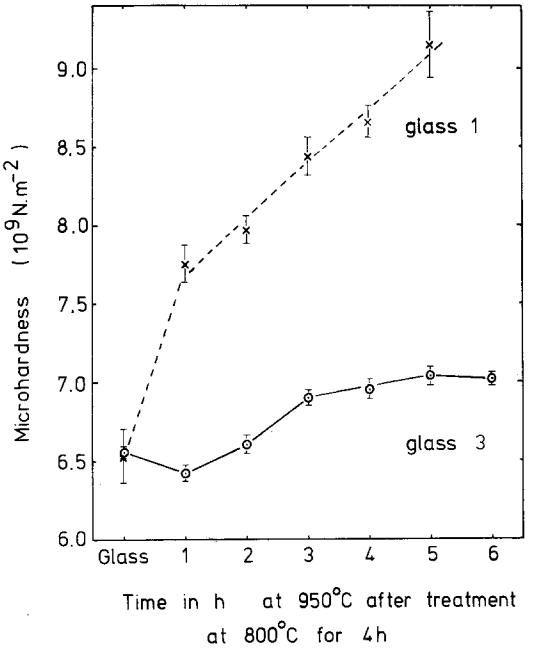

Figure 9 Comparison of microhardness of glasses 1 and 3 after various heat treatment times.

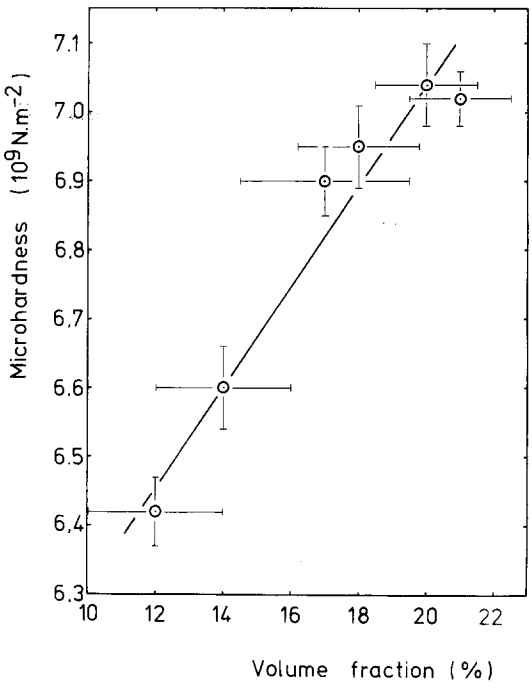

Figure 10 Variation of microhardness, H_v, with volume fraction, V_f, of gahnite crystals in glass-ceramic 3.

3.3. Optical properties.

Optical transmission properties were measured for glasses and glass-ceramics 1, 2, 3 and 4 of 1 mm thickness. The overall transparency in the visible and near infra-red regions appears to be very good.

In the near infra-red region, similar spectra were obtained for all the above glasses. Fig. 12 shows the percentage transmission. The absorption peak at 2.8 μm is assigned to vibrations of –OH group linked to non-bridging oxygen ions, indicating a presence of physically absorbed water either in the glass or on the surface [11–14]. The 4.25 μm peak is due to $(CO_3)^{2-}$ [15]. The small point of inflexion at 4.5 μm is due to the overtone of the fundamental vibration of SiO_4 tetrahedra occur-

TABLE V Microhardness of glasses and glass-ceramics

Composition no.	Base glass		Glass-ceramic 800° C 4 h–900° C 4 h	
	H_v (kg mm^{-2}) VHN	H_v (10^9 N m^{-2})	H_v (kg mm^{-3}) VHN	H_v (10^9 N m^{-2})
1	666 ± 17	6.53 ± 0.17	883 ± 10	8.66 ± 0.10
2	688 ± 5	6.73 ± 0.05	789 ± 7	7.74 ± 0.07
3	669 ± 3	6.56 ± 0.03	709 ± 6	6.95 ± 0.06
4	642 ± 8	6.30 ± 0.08	749 ± 6	7.35 ± 0.06

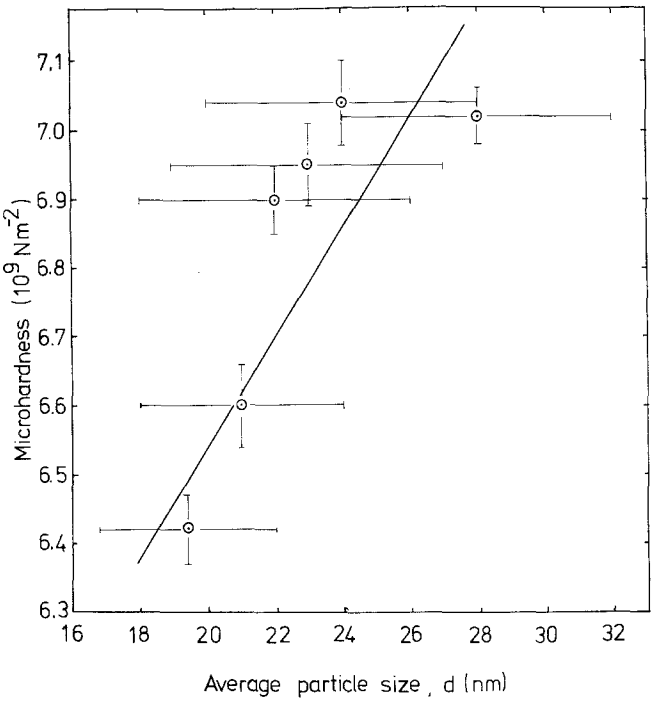

Figure 11 Dependence of microhardness upon the average particle size, d, for glass-ceramic 3.

ring at 9 μm. Following this the transmission cut-off at approximately 5 μm is, as expected, due to the extremely strong absorption of the Si–O network.

Fig. 13 shows the percentage transmission of the above glasses and glass-ceramics in the visible range. All the parent glasses have a very similar transmission of around 80% over the complete range. The glass-ceramics vary somewhat with glass-ceramic 8 having a more translucent appearance, and thus having the least transmission. For all the glasses and glass-ceramics, the cut-on in the ultra-violet region occurs at around 250 nm, which ties in fairly well with the well-known observation that transition metal impurities commonly found in glass produce absorption in the ultra-violet region, depending on the valence state of the impurity ions [6].

Glass 2 has the greater absorption towards the u.v. possibly because the concentration of impurities such as iron and manganese is greatest in the MgO used to prepare glass 2, compared to the other alkaline earth metal oxides, CaO and BaO used to prepare the other glasses.

4. Discussion

The various physical properties of the glass-ceramics have in general shown to be strongly dependent on the time held at the crystallization temperature. It is of interest to consider how far these variations are explainable in terms of the microstructural changes.

It was notable [1] that a number of properties of glass-ceramic 3 attain a maximum or minimum value for glass-ceramics produced by a crystallization heat treatment at a temperature of 950° C for a time of 5 to 6 h.

No distinct maximum value was noted either for the volume fraction or the particle size after this time, but microstructural analysis by TEM showed no change in the quantities after 24 h at 950° C. Because of the difficulty in measurement of the microstructural properties, no conclusive evidence can be given regarding direct relationships. But because of the diverse nature of the properties studied, it seems reasonable to suppose that these observations are explainable, at least partly in terms of microstructural effects.

It should be recalled [1] at this point that a detailed analysis of the microstructure of glass-ceramic 3 showed the volume fraction of the crystalline phase to have attained a flattened maximum and the mean free path in the residual glass phase, λ, a distinct minimum for the material heat treated at 950° C for 5 h, after a nucleation treatment at 800° C for 4 h.

Firstly, the thermal expansion of glass 3 appears to be microstructure sensitive. These properties increase just as the volume fraction of gahnite crystals increases and then level off to a stable

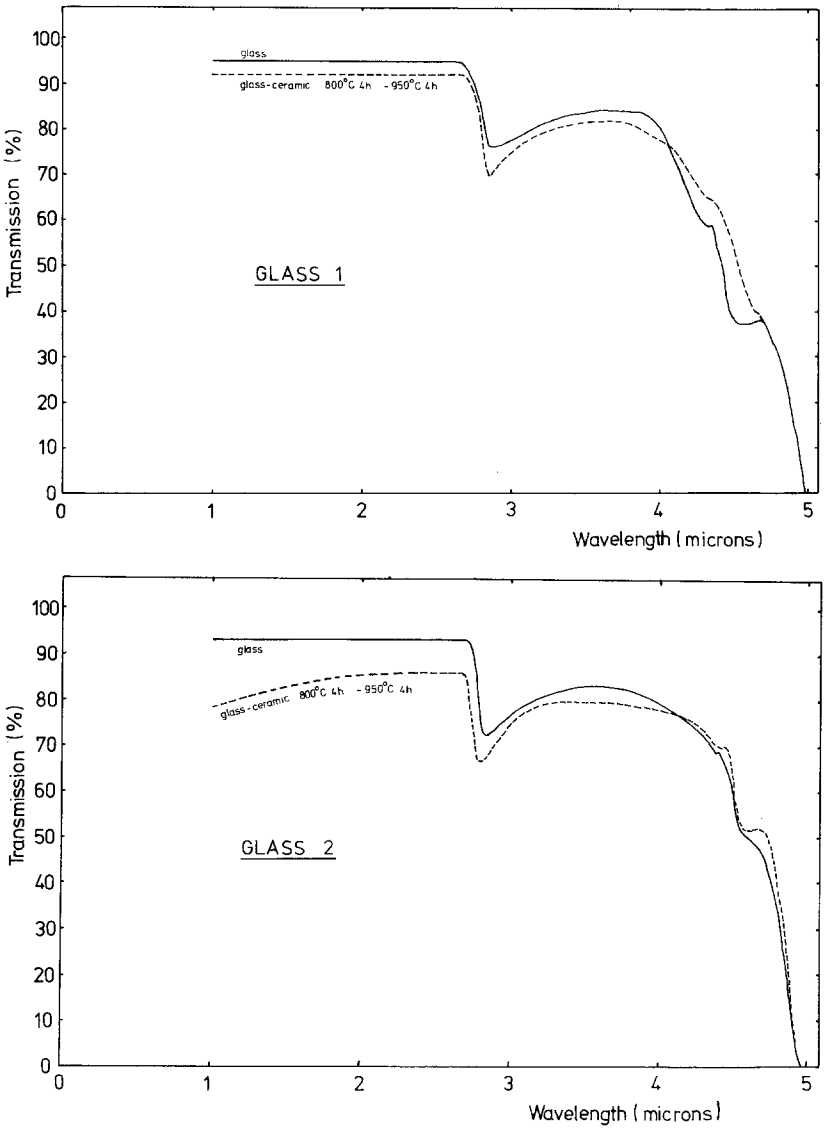

Figure 12 Infra-red spectra of glasses and glass-ceramics 1, 2, 3, and 4.

value after 5 to 6 h at the crystallization temperature. The presence of larger alkaline earth metal ions increases the expansion coefficient quite significantly.

A wide range of thermal expansions can be obtained, depending on the crystalline phases and the alkaline earth metal ions present.

The microhardness of glass-ceramic 3 gradually increases during heat treatment until a flattened maximum is reached, which again coincides with a maximum volume fraction and minimum mean free path. The microhardness has been shown to depend on the particle size, which indicates that the deformation process is related to slip occurring in the glass terminated by the crystal boundaries.

The maximum strength occurs within one hour of the crystallization treatment where the minimum particle size occurs. Analysis of the results established a linear relationship between the modulus of rupture and $d^{-1/2}$ and supported the view that the strength of the glass-ceramic is controlled by microflaws present at the glass–crystal interface, due to thermal expansion mismatch producing stresses at the interface.

The Young's modulus increases from the parent glass to the glass-ceramic and remains constant over the complete crystallization heat treatment.

When attempting to compare the optical properties in the visible region of the glass-ceramics to the microstructure, especially particle size, difficulty arises in explaining the loss of transmission in the blue region due to light scattering. The particle size of the crystals in all the glasses heat treated at 800° C for 4 h and 950° C for 4 h, was

Figure 12 Continued.

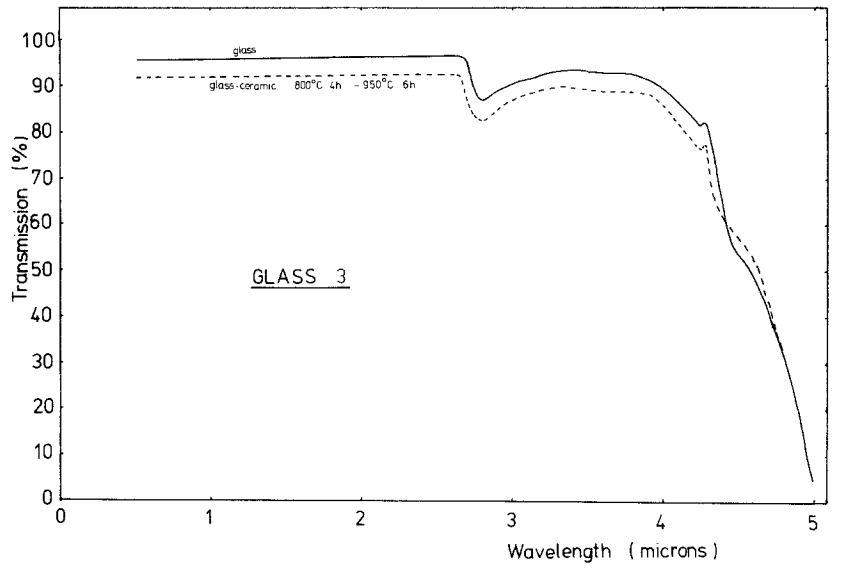

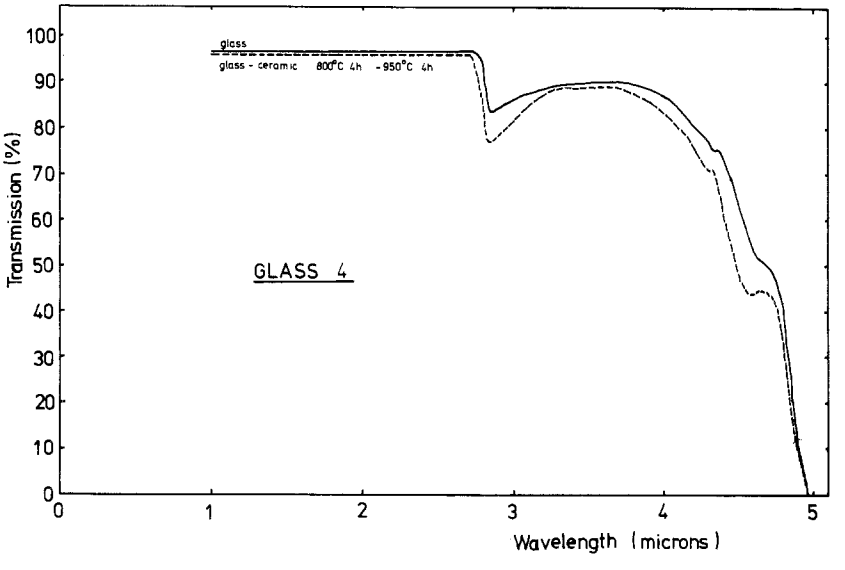

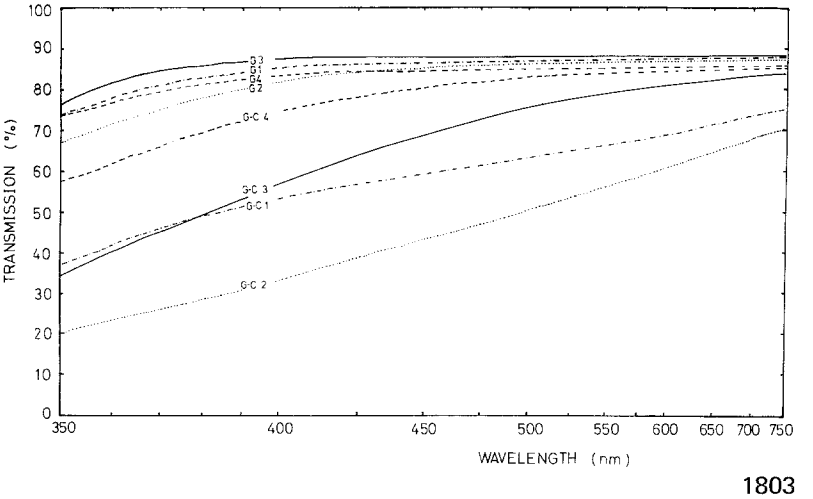

Figure 13 Visible spectra of glass and glass-ceramics 1, 2, 3, and 4.

much smaller than the wavelength of light, and in any case varied from 10 to 23 nm. This makes the explanation of why there is such a large variation in the transmission of the glass-ceramics very difficult. Glass-ceramics 1 and 2 have the worst transmissions and it can be pointed out that after the nucleation heat treatment, these materials had a bluish appearance, indicating light scattering was occurring. The micrographs of glass-ceramic 2 [1], showed that in the nucleation stage, a background phase separation of the order of 100 nm was present, but no sign of this was apparent after the crystallization stage. The only explanation that can be offered relates to the presence of larger quantities of impurities in the MgO in glass-ceramics 1 and 2, but this would also decrease the transmission in the parent glasses.

Acknowledgement

The authors would like to thank the SRC and Thorn Lighting Ltd. for the provision of a CAPS award.

References

1. A. J. STRYJAK and P. W. McMILLAN, *J. Mater. Sci.* **13** (1978) 1275.
2. J.C. BAILAR, "Comprehensive Inorganic Chemistry", Vol. 1 (Pergamon Press, Oxford, 1973).
3. *Idem, ibid.*, Vol. 3.
4. National Research Council, "International Critical Tables" (McGraw Hill, New York, 1926).
5. R. N. HAWARD, "Strength of Plastics and Glass" (Cleaver-Hume Press, London, 1949).
6. M. TASHIRO and S. SAKKA, *Glass Ind.* **47** (1966) 428.
7. P. W. McMILLAN, Proceedings of the Xth International Conference on Glass, Vol. 14 (1974) 1.
8. LANDOLT-BÖRNSTEIN, "Numerical Data and Functional Relationships" (Springer-Verlag, Berlin, 1950).
9. A. N. STROH, *Phil. Mag.* **46** (1955) 968.
10. C . M. ZENER, "Elasticity and Anelasticity of Metals" (University of Chicago Press, 1952) p. 154.
11. F. W. GLAZE, J. M. FLORENCE, C. H. HAHNER and R. STAIR, *J. Amer. Ceram. Soc.* **31** (1948) 328.
12. F. W. GLAZE, C. C. ALLHOUSE, J. M. FLORENCE and C. H. HAHNER, *J. Res. Nat. Bur. Stand.* **45** (1950) 121.
13. F. W. GLAZE, M. H. BLACH and J. M. FLORENCE, *ibid.* **50** (1953) 187.
14. F. W. GLAZE, *Bull Amer. Ceram. Soc.* **34** (1955) 291.
15. R. V. ADAMS, *Phys. Chem. Glasses* **2** (1961) 39.
16. G. H. SIGEL and R. J. GINTHER, *J. Non-Cryst. Solids* **13** (1974) 372.

Received 14 November and accepted 19 December 1977.